Biochemical and Biophysical Research Communications 444 (2014) 109–115

Contents lists available at ScienceDirect

Biochemical and Biophysical Research Communications

journal homepage: www.elsevier.com/locate/ybbrc

Crystal structure of FliC flagellin from *Pseudomonas aeruginosa* and its implication in TLR5 binding and formation of the flagellar filament ☆

Wan Seok Song, Sung-il Yoon *

Department of Systems Immunology and Institute of Antibody Research, College of Biomedical Science, Kangwon National University, Chuncheon 200-701, Republic of Korea

ARTICLE INFO

Article history:
Received 24 December 2013
Available online 14 January 2014

Keywords:
Pseudomonas aeruginosa
Flagellin
FliC
Structure
TLR5
Flagellar filament

ABSTRACT

Pseudomonas aeruginosa is one of leading opportunistic pathogens in humans and its movement is driven by a flagellar filament that is constituted through the polymerization of a single protein, FliC flagellin (paFliC). paFliC is an essential virulence factor for the colonization of *P. aeruginosa*. paFliC activates innate immune responses via its recognition by Toll-like receptor 5 (TLR5) and adaptive immunity in the host. Thus, paFliC has been a vaccine candidate to prevent *P. aeruginosa* infection, particularly for cystic fibrosis patients. To provide structural information on paFliC and its flagellar filament, we have determined the crystal structure of paFliC, which contains the conserved D1 and variable D2 domains, at 2.1 Å resolution. As observed for *Salmonella* FliC, the paFliC D1 domain is folded into a rod-shaped structure, and paFliC was demonstrated by gel filtration and native PAGE analyses to directly interact with TLR5. Moreover, a structural model of the paFliC-TLR5 complex suggests that paFliC D1 would provide major TLR5-binding sites, similar to *Salmonella* FliC. In contrast to the D1 domain, the paFliC D2 domain exhibits a unique structure of two β-sheets and one α-helix that has not been found in other flagellins. An *in silico* construction of a flagellar filament based on the packing of paFliC in the crystal suggests that the D2 domain would be exposed to solution and could play an important role in immunogenicity. Our biophysical and structure-based modeling study on paFliC, the paFliC-TLR5 complex, and the paFliC filament could contribute to the improvement of vaccine design to control *P. aeruginosa* infection.

1. Introduction

Pseudomonas aeruginosa is a Gram-negative bacterium that is ubiquitously found in the environment including soil and water [1]. *P. aeruginosa* is a major opportunistic human pathogen that is responsible for severe hospital- and community-acquired infections in the urinary tract, the kidney, the lung, the cornea, and surgical or burn wounds [2,3]. *P. aeruginosa* is a major cause of life-threatening lung infections in cystic fibrosis (CF) patients and ~76% of adult CF patients are colonized by *P. aeruginosa* [4]. *P. aeruginosa* is motile with a single polar flagellum that contributes to infection as a virulence factor by facilitating bacterial adhesion to host cells or wet surfaces [5].

Bacterial flagella are anchored to the cell wall and membrane through the basal body that extends to the filament via the hook [6,7]. The flagellar filament is composed of a single protein, flagellin. Structural studies on the flagellar filament from *Salmonella enterica* subspecies *enterica* serovar Typhimurium (*Salmonella* Typhimurium) demonstrated that the filament is produced through the longitudinal assembly of 11 protofilaments, each of which forms as a result of vertical polymerization of flagellin monomers [8–10].

Flagellin has a mass of 28–65 kDa and contains at least two domains [8–10]. The two essential domains, defined as D0 and D1 in FliC (a flagellin gene product) from *S.* Typhimurium (stFliC), mediate intersubunit interactions in the flagellar filament and, thus, share high sequence identity with other flagellins. The D0 and D1 domains are assembled into a double-tubular structure and form the inner and outer rings, respectively. stFliC contains two additional domains, D2 and D3, that project from the D0–D1 tubular structure without significant contribution to intersubunit interactions in the filament. The D2 and D3 domains exhibit high sequence variation, potentially due to a lack of evolutionary restraint, and are even absent in some species, such as *Bacillus subtilis* [9,11].

When pathogenic flagellated bacteria infect the host, flagellin is detected as a pathogen-associated molecular pattern by innate immune receptors, including Toll-like receptor 5 (TLR5) and

☆ Data deposition: The atomic coordinates and structure factors for paFliC-ΔD0 have been deposited in the Protein Data Bank, www.pdb.org (PDB ID 4NX9).

* Corresponding author. Address: 1 Kangwondaehak-gil, Biomedical Science building A-204, Chuncheon 200-701, Republic of Korea. Fax: +82 33 250 8380.
E-mail address: sungil@kangwon.ac.kr (S.-i. Yoon).

0006-291X/$ - see front matter © 2014 Elsevier Inc. All rights reserved.
http://dx.doi.org/10.1016/j.bbrc.2014.01.008

NAIPs/NLRC4, which elicit potent immune responses against pathogens [12,13]. In addition to the role in immune stimulation, flagellin exerts radioprotective activity upon the hematopoietic system and gastrointestinal tissues through TLR5 activation [14]. Thus, flagellin has been applied to develop new vaccines as adjuvants against influenza, West Nile fever, malaria, and tuberculosis, as well as anti-radiation therapeutics [15–18].

TLR5 is a type I receptor that consists of an N-terminal extracellular domain, a single-pass transmembrane domain, and a C-terminal intracellular domain. The extracellular domain of TLR5 is folded into a curved leucine-rich repeat (LRR) domain structure and is responsible for direct interaction with flagellin from β- and γ-proteobacteria of Gram-negative bacteria and some Gram-positive bacteria [11,19]. Structural studies on the interaction between the N-terminal 14 LRR modules of *Danio rerio* TLR5 (TLR5-N14) and the D1–D2 domains of *Salmonella* Dublin FliC (sdFliC) revealed that TLR5 interacts with the highly conserved residues of the sdFliC D1 domain that are buried within the flagellar filament [11,19,20]. Flagellin organizes two TLR5 chains into a tail-to-tail assembly through high-affinity 1:1 'primary binding' and subsequent low-affinity 'secondary dimerization' of two 1:1 complexes into a 2:2 complex.

FliC flagellin from *P. aeruginosa* (paFliC) activates innate immunity as a TLR5 agonist and promotes adaptive immune responses as an antigen [21,22]. Thus, paFliC has been one of the major targets for vaccine and therapeutic development in particular for CF patients. For example, *P. aeruginosa* flagella were developed as a vaccine against *P. aeruginosa* and significantly lowered the risk for initial *P. aeruginosa* infection in CF patients in a phase III study [23]. A fusion protein of the *P. aeruginosa* OprF fragment, OprI, and FliC promoted the clearance of *P. aeruginosa* in a pulmonary challenge model [24]. Furthermore, topical administration of paFliC protects injured cornea from *P. aeruginosa* infection by activating the corneal innate immune response in the mouse system [25]. To improve vaccine design and to define its action mechanism, structural information on paFliC and its flagellar filament are required, and the paFliC-TLR5 binding mode must be investigated.

Here, we report the crystal structure of D0-deleted paFliC (paFliC-ΔD0), which contains the D1 and D2 domains, at 2.1 Å resolution. In contrast to the conserved D1 domain, the D2 domain of paFliC adopts a unique structure that has not been observed in other flagellum-forming flagellins. Based on our modeling study on the paFliC filament, we propose that the variant D2 domain could function as an immunogenic determinant.

2. Materials and methods

2.1. Expression and purification of paFliC and TLR5-N14

To generate the paFliC-ΔD0 expression vector, paFliC-ΔD0 (residues 55–341) from the a-type FliC gene of *P. aeruginosa* (ATCC 15522) was amplified using PCR and ligated to a modified pET49b vector that contained the N-terminal His_6 tag and thrombin cleavage site.

Selenomethionine-incorporated paFliC-ΔD0 (SeMet-paFliC-ΔD0) proteins were expressed using an *Escherichia coli* B834 (DE3) strain that contained the paFliC-ΔD0 expression vector. Cells were grown at 37 °C in M9 minimal medium (Molecular Dimensions) containing 50 μg/ml kanamycin and 40 μg/ml L-SeMet. Protein expression was induced at an OD_{600} (optical density at 600 nm) of ~0.8 using 1 mM IPTG and continued for 3 h at 37 °C. The Cells were then collected using centrifugation. SeMet-paFliC-ΔD0 was initially purified by Ni–NTA affinity chromatography, and the N-terminal His_6 tag was removed using thrombin. The resultant proteins were further purified by anion exchange chromatography.

Danio rerio TLR5-N14 proteins that contained the N-terminal capping motif to LRR14 were expressed in the baculovirus expression system and purified by Ni–NTA affinity, Strep-Tactin affinity, and gel filtration chromatography, as previously described [11,20].

2.2. Crystallization of paFliC-ΔD0 and X-ray data collection

SeMet-paFliC-ΔD0 was crystallized in a drop containing 0.5 μl of 16.7 mg/ml protein and 0.5 μl of 22% (*w*/*v*) PEG6000/0.1 M bicine, pH 9.0/8% 2,2,2-trifluoroethanol at 18 °C by the sitting drop vapor diffusion method. The crystals were flash-frozen in 25% (*w*/*v*) PEG6000/0.1 M bicine, pH 9.0/8% 2,2,2-trifluoroethanol/25% ethylene glycol under cryo-stream at 100 K. X-ray diffraction data were collected at beamline 7A of the Pohang Accelerator Laboratory (Korea). Diffraction data were reduced and scaled using the *HKL2000* package [26].

2.3. Structure determination of paFliC-ΔD0

The paFliC-ΔD0 structure was determined by single-wavelength anomalous diffraction (SAD) phasing. Selenium sites were identified and refined using *AutoSol* in the *Phenix* program [27]. Phase calculation and modification were performed using *AutoSol*. The initial paFliC-ΔD0 model was obtained using *AutoBuild* in the *Phenix* program. Iterative model building and refinement were carried out using the *Coot* and *Refmac5* programs, respectively, and yielded a high quality structure of paFliC-ΔD0 [28,29].

2.4. Analysis of paFliC-ΔD0:TLR5-N14 binding

To examine the formation of a complex between paFliC-ΔD0 and TLR5-N14, gel filtration chromatography was performed using a Superdex 200 10/300 column in running buffer consisting of 20 mM Hepes, pH 7.4/150 mM NaCl. 14 μg of paFliC-ΔD0, 24 μg of TLR5-N14, or their mixture at a 1:1 molar ratio was injected into the column and the elution profile was recorded by monitoring the UV absorbance at 280 nm.

To analyze the interaction, native polyacrylamide gel electrophoresis (PAGE) was carried out using 6% polyacrylamide gels at pH 8.8. 10 μl of each sample (paFliC-ΔD0, TLR5-N14, and their mixture) was loaded into a native gel and electrophoresed at 100 V for 1.5 h. The gel was stained with Coomassie brilliant blue.

3. Results and discussion

3.1. The Overall structure of paFliC-ΔD0

FliC from *P. aeruginosa* strain ATCC 15522 (paFliC) consists of three domains (D0, D1, and D2) (Fig. 1A). The crystal structure of paFliC-ΔD0 containing the D1 and D2 domains was determined by SAD phasing using a crystal of SeMet-incorporated proteins (residues 55–341) and was refined at 2.1 Å resolution. Data collection, phasing, and refinement statistics are shown in Table S1. The asymmetric unit contains one paFliC-ΔD0 molecule (residues 58–334).

The paFliC-ΔD0 structure is composed of two domains: D1 (residues 58–168 and residues 285–334) and D2 (residues 169–284) (Fig. 1). The D1 domain is folded into an ~70 Å-long rod that is constructed from two discontinuous segments, the N-terminal portion ($D1^N$) of two α-helices (αD1a and αD1b) and two β-strands (βD1a and βD1b), and the C-terminal portion ($D1^C$) of an α-helix (αD1c). Two long α-helices (40-residue αD1a and 41-residue αD1c) and a shorter α-helix (24-residue αD1b) form one side of the rod and

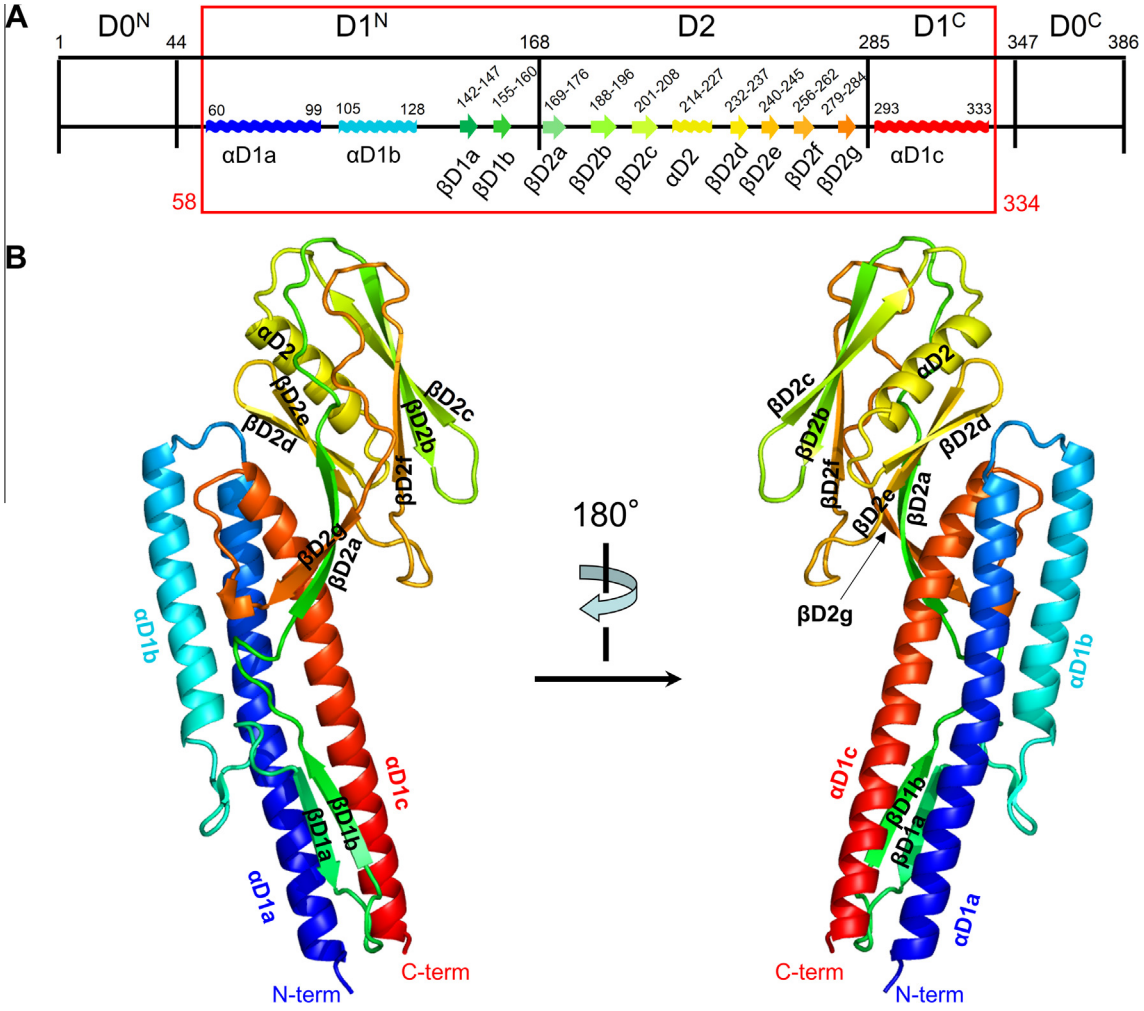

Fig. 1. The domain organization and crystal structure of paFliC-ΔD0. (A) Schematic representations of the domain structures and secondary structure elements in paFliC. α-helices and β-strands (>3 residues) are represented by waves and arrows, respectively. Domain boundary residues and terminal residues of each secondary structure are labeled in black. The protein region that was built in the paFliC-ΔD0 structure is highlighted by a red box with terminal residue numbers shown in red. (B) The paFliC-ΔD0 structure in rainbow ribbons from the N-terminus in blue to the C-terminus in red. Secondary structures are labeled. (For interpretation of the references to colour in this figure legend, the reader is referred to the web version of this article.)

are supported on the back by two β-strands (βD1a and βD1b) and random coils.

The D2 domain adopts a cup-like structure consisting of two β-sheets (βD2g-a-e-d and βD2f-b-c) with a handle (Fig. 1B). The top of the cup is closed by one α-helix (αD2) that is embraced by βD2c and βD2d at the entrance (Fig. 1B right). The bottom of the cup comprises βD2f, βD2f-g loop, the N-terminal part of βD2a, and βD2a-b loop, and is connected to the side of the D1 rod through the handle of βD2a and βD2g (Fig. 1B left). The exterior surface of the βD2g-a-e-d sheet contacts the N-terminal residues of αD1c and buries a surface area of ~550 Å^2. The relative orientation of paFliC D1 and D2 seems to be inflexible, given that another paFliC-ΔD0 structure in a different space group showed an essentially identical D1–D2 inter-domain angle (data not shown).

3.2. Structural comparison of paFliC-ΔD0 with its homologues

In addition to our paFliC structure, two types of FliC, including stFliC and sdFliC (PDB ID, 3A5X and 3V47, respectively), have been structurally characterized. Comparative analysis revealed a common conserved structure in the D1 domain but distinct features in the variable D2 domain. The paFliC D1 domain exhibits high similarities in structure and sequence to those of stFliC and sdFliC with root mean square deviation (RMSD) values of ~1.1 Å (~140 from 148 D1 residues) and sequence identities of 45–47% (Figs. 2A and S1). In contrast, the paFliC D2 domain shows several unique structural features compared with those of stFliC and sdFliC (Fig. 2A). First, each D2 domain of the currently available flagellin structures presents a completely different fold, as expected from the high sequence variation of the D2 domains. Second, paFliC connects D1 and D2 in a different mode. D2 of paFliC extends from the side of the D1 domain through a handle structure, whereas each D2 domain of stFliC and sdFliC directly stacks on the top of the D1 domain (the box of Fig. 2A). Third, we observed positional differences of the D2 domains when the D1 domains were superimposed. paFliC D2 and stFliC D2 are placed in opposite directions with respect to D1, and sdFliC D2 is positioned on the top of D1.

Because the structural fold of paFliC D2 has not been observed in filament-forming flagellins, structural homologues of paFliC D2 were searched using the Dali server. In the search list, p5 (PDB ID, 2ZBI) of *Sphingomonas* sp. A1 was found to be the most homologous to paFliC D2 with an RMSD value of 2.75 Å (87 from 116 residues). p5 is a cell surface protein of *Sphingomonas* sp. A1, and does not seem to be involved in the formation of a flagellar filament, which was expected because *Sphingomonas* sp. A1 is not motile. p5 functions in the recognition and transport of alginate

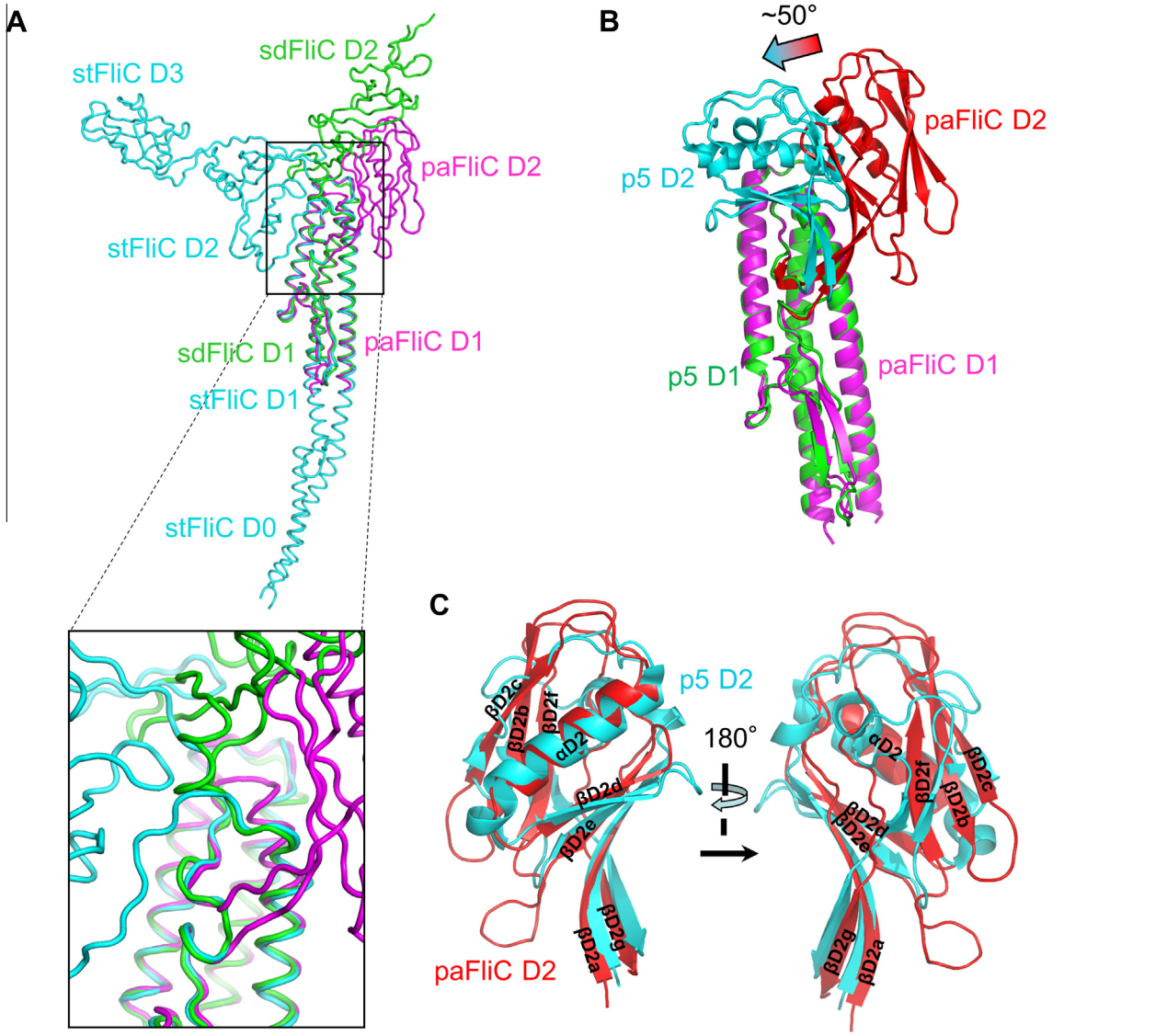

Fig. 2. Structural comparison of paFliC with its homologues. (A) Structural comparison of paFliC-ΔD0 (magenta) with stFliC (cyan; PDB ID 3A5X) and sdFliC-ΔD0 (green; PDB ID 3V47). The D1 domains were superimposed. (B) Structural comparison of paFliC-ΔD0 (D1, magenta; D2, red) and p5-ΔD0 (D1, green; D2, cyan; PDB ID 2ZBI). The D1 domains were superimposed. (C) Structural comparison of paFliC D2 (red) and p5 D2 (cyan). The D2 domains were superimposed. (For interpretation of the references to colour in this figure legend, the reader is referred to the web version of this article.)

polysaccharides into the cell [30,31]. Although p5 and paFliC mediate unrelated functions, both contain three domains of D0–D1–D2 and exhibit structural resemblance within each domain, especially in D1 (RMSD, 0.73 Å for 147 from 161 residues) (Fig. 2B). The paFliC and p5 D2 domains share similar secondary structure organization that consists of two β-sheets and one α-helix (Fig. 2C). The β-sheet (βD2g-a-e-d) that is closer to D1 is similar in length and organization of its β-strands. However, the other β-sheet (βD2f-b-c) of paFliC is composed of three long β-strands, whereas the counterpart of p5 consists of four short β-strands. Another distinct feature is the D1–D2 inter-domain angle (Fig. 2B). D2 of p5 rotates toward the top of the D1 domain by ~50° from paFliC D2 using the pivot of the D1–D2 connecting region.

3.3. Interaction of paFliC with TLR5

paFliC activates TLR5-mediated cellular responses [21]. However, the direct interaction between paFliC and TLR5 has not been characterized. To examine the paFliC-TLR5 interaction, we carried out gel filtration chromatography and native PAGE using paFliC-ΔD0 and TLR5-N14 (Fig. 3A and B). In gel filtration chromatography, a mixture of paFliC-ΔD0 and TLR5-N14 eluted earlier than each component, suggesting complex formation (Fig. 3A). In native PAGE analysis, paFliC-ΔD0 and TLR5-N14 shifted to a new band that corresponded to their complex (Fig. 3B). Complete complex formation was observed at a 1:1 molar ratio, suggesting a 1:1 paFliC:TLR5 binding stoichiometry, similar to sdFliC:TLR5 [11].

Based on the high sequence and structure similarities of paFliC D1 and sdFliC D1, a paFliC-TLR5 binding model was generated by superimposing paFliC D1 on the structure of the 2:2 sdFliC-ΔD0:TLR5-N14 complex (Fig. 3C) [11]. paFliC forms a 2:2 complex with TLR5-N14 without major steric clashes. The D2 domain of paFliC is located above D1 away from the binding interfaces and does not contact any TLR5 chains or the other paFliC molecule. In contrast, paFliC D1 forms primary binding and secondary dimerization interfaces, as observed for sdFliC D1. Three α-helices of paFliC D1 provide major binding sites for TLR5, and the R90 and E114 residues of paFliC αD1a are located at a core interaction site. The

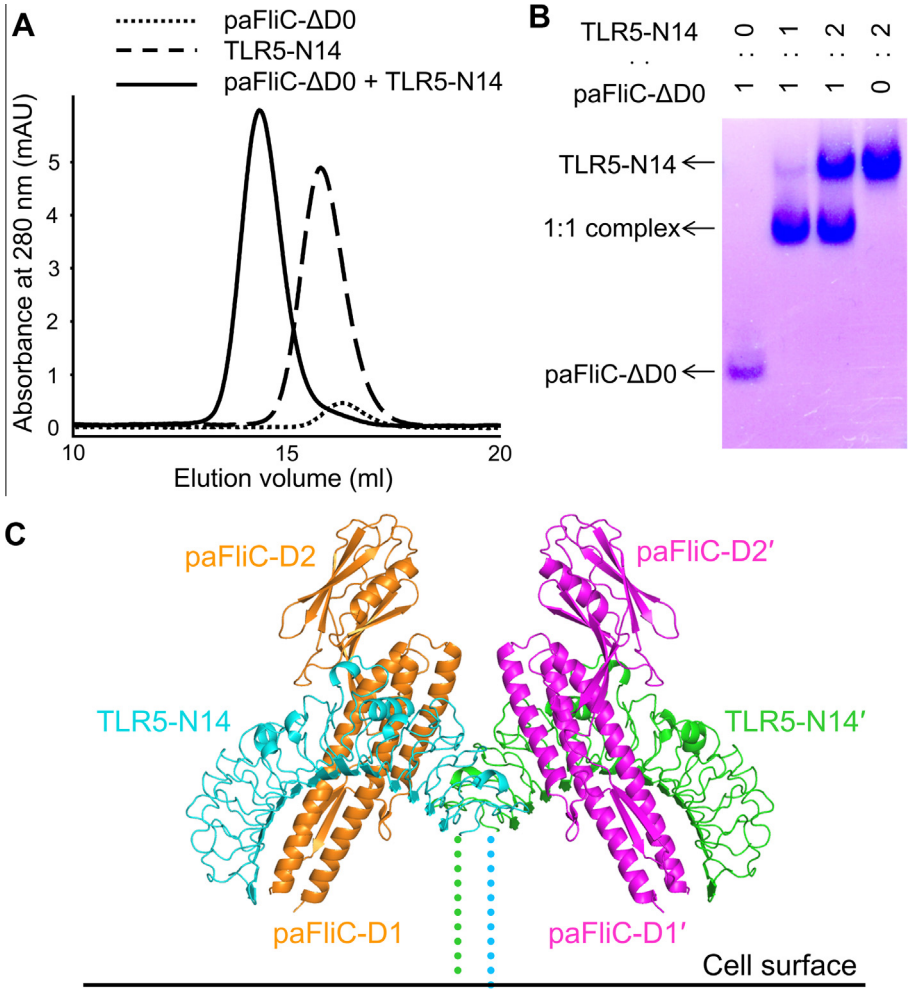

Fig. 3. TLR5-N14 interactions with paFliC. (A) Gel filtration chromatography analysis of paFliC-ΔD0:TLR5-N14 complex formation using a Superdex 200 10/300 column. (B) Native PAGE analysis of paFliC-ΔD0:TLR5-N14 complex formation. (C) A proposed model of paFliC-ΔD0 in complex with TLR5-N14. sdFliC of the 2:2 sdFliC-ΔD0:TLR5-N14 complex (PDB ID 3V47) was replaced with paFliC by superposition of the D1 domains. The paFliC molecules are colored in orange and magenta. TLR5 chains are shown in cyan and green, and the C-terminal regions that are not built into the structure are represented by broken lines. (For interpretation of the references to colour in this figure legend, the reader is referred to the web version of this article.)

binding model, along with the high conservation (61%) of the sdFliC interface residues in paFliC (22 of 36 interface residues) (Fig. S1), suggests that paFliC and sdFliC share a similar TLR5 binding mechanism.

3.4. Flagellar filament model from the paFliC structure

Although the asymmetric unit of the paFliC crystal contains one paFliC molecule, vertically aligned paFliC molecules in the crystal packing form a continuous polymer chain that mimics the stFliC protofilament (Fig. S2), providing a paFliC protofilament model. Intersubunit binding in the paFliC protofilament model is mediated by a combination of D1–D1′ and D2–D1′ interactions with buried surface areas of 680 and 450 Å^2, respectively (Figs. 4A and S3A). The D1–D1′ interaction is conserved in the paFliC and stFliC protofilaments. However, a significant contribution of the variable D2 domain to paFliC protofilament formation has not been observed in stFliC protofilaments. The unique role of D2 in the paFliC protofilament was further supported by the conservation of binding interface residues in flagellins of diverse *Pseudomonas* species (Fig. S3B).

High sequence identity (~50%) of the D0–D1 domains between paFliC and stFliC, combined with the observation that vertical alignment of the stFliC molecules in the protofilament is recapitulated in the crystal packing of paFliC, suggests that both flagellins would form a flagella filament in a conserved manner. The molecular architecture of the paFliC filament was modeled by superimposing paFliC D1 on the cryo-electron microscopy structure of the stFliC filament (Fig. 4B and C). No significant steric clashes were observed in the paFliC filament model, indicating the reliability of the model. The paFliC D1 domains occupy the tubule of the filament with three D1 α-helices buried inside the filament (a view on Fig. 1B right) and the other side of the two β-strands faced outwards (a view on Fig. 1B left). In the paFliC D2 domain, the top of the D2 cup at βD2c, αD2, and βD2d is buried into the filament. However, the other side (βD2a, βD2b, βD2a-b loop, βD2f, βD2e-f loop, βD2g, and βD2f-g loop) at or near the bottom of the cup is exposed to solution (Fig. 4D), suggesting that they would function as major epitopes for antibodies that would be produced by a flagella vaccine against *P. aeruginosa* for CF patients. Another distinct feature of the paFliC filament is that its diameter (~15 nm) is smaller than that of the stFliC filament (~24 nm) since paFliC lacks the D3 domain and its D2 domain protrudes less (Fig. 4B and C). In conclusion, our structural and modeling study proposes a critical role for the variable D2 domain of paFliC in forming a flagellar filament and eliciting immunogenicity.

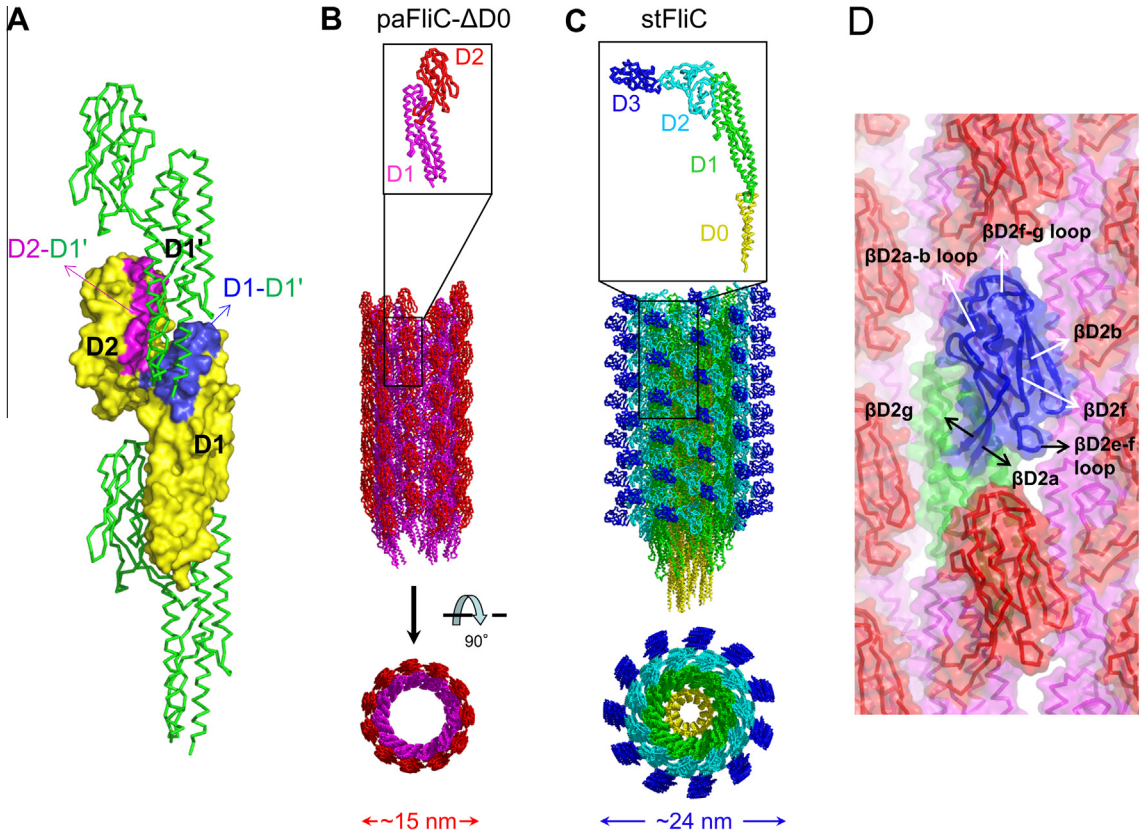

Fig. 4. A proposed model of a flagellar filament from *P. aeruginosa* compared with the stFliC filament. (A) Intermolecular contacts of paFliC formed by vertically aligned paFliC molecules in the crystal lattice provide the basis on a paFliC-ΔD0 protofilament model. The D1–D1′ and D2–D1′ binding interfaces are colored in blue and magenta, respectively, on the surface representation of a paFliC molecule located in the center. (B) A model of a paFliC filament (middle, a side view of the filament; bottom, a cross-section view of the filament) with the structure of the paFliC-ΔD0 monomer (top). paFliC D1 and D2 are colored in magenta and red, respectively. (C) Cryo-electron microscopy structure of the stFliC filament (PDB ID 3A5X). The D0, D1, D2, and D3 domains of stFliC are colored in yellow, green, cyan, and blue, respectively. (D) Exposed regions (βD2a, βD2b, βD2a-b loop, βD2f, βD2e-f loop, βD2g, and βD2f-g loop) of D2 in the paFliC-ΔD0 filament model. D1 and D2 of the paFliC-ΔD0 molecule in the center are colored in blue and green, respectively, and its surrounding paFliC-ΔD0 molecules are in red and magenta. (For interpretation of the references to colour in this figure legend, the reader is referred to the web version of this article.)

Acknowledgments

X-ray diffraction datasets were collected at the Pohang Accelerator Laboratory beamline 7A, and we thank beamline staff members. This study was supported by Basic Science Research Program through the National Research Foundation of Korea (NRF) funded by the Ministry of Education, Science and Technology (2012R1A1A1003701 to SIY) and by 2012 Research Grant from Kangwon National University (to SIY).

Appendix A. Supplementary data

Supplementary data associated with this article can be found, in the online version, at http://dx.doi.org/10.1016/j.bbrc.2014.01.008.

References

[1] C. Hardalo, S.C. Edberg, *Pseudomonas aeruginosa*: assessment of risk from drinking water, Crit. Rev. Microbiol. 23 (1997) 47–75.
[2] J.A. Driscoll, S.L. Brody, M.H. Kollef, The epidemiology, pathogenesis and treatment of *Pseudomonas aeruginosa* infections, Drugs 67 (2007) 351–368.
[3] A.A. El Solh, A. Alhajhusain, Update on the treatment of *Pseudomonas aeruginosa* pneumonia, J. Antimicrob. Chemother. 64 (2009) 229–238.
[4] B. Wiedemann, G. Steinkamp, B. Sens, M. Stern, G. German cystic fibrosis quality assurance, the German cystic fibrosis quality assurance project: clinical features in children and adults, Eur. Respir. J. 17 (2001) 1187–1194.
[5] H.C. Ramos, M. Rumbo, J.C. Sirard, Bacterial flagellins: mediators of pathogenicity and host immune responses in mucosa, Trends Microbiol. 12 (2004) 509–517.
[6] K. Yonekura, S. Maki-Yonekura, K. Namba, Growth mechanism of the bacterial flagellar filament, Res. Microbiol. 153 (2002) 191–197.
[7] R.M. Macnab, Genetics and biogenesis of bacterial flagella, Annu. Rev. Genet. 26 (1992) 131–158.
[8] S. Maki-Yonekura, K. Yonekura, K. Namba, Conformational change of flagellin for polymorphic supercoiling of the flagellar filament, Nat. Struct. Mol. Biol. 17 (2010) 417–422.
[9] F.A. Samatey, K. Imada, S. Nagashima, F. Vonderviszt, T. Kumasaka, M. Yamamoto, K. Namba, Structure of the bacterial flagellar protofilament and implications for a switch for supercoiling, Nature 410 (2001) 331–337.
[10] K. Yonekura, S. Maki-Yonekura, K. Namba, Complete atomic model of the bacterial flagellar filament by electron cryomicroscopy, Nature 424 (2003) 643–650.
[11] S.I. Yoon, O. Kurnasov, V. Natarajan, M. Hong, A.V. Gudkov, A.L. Osterman, I.A. Wilson, Structural basis of TLR5-flagellin recognition and signaling, Science 335 (2012) 859–864.
[12] E.M. Kofoed, R.E. Vance, Innate immune recognition of bacterial ligands by NAIPs determines inflammasome specificity, Nature 477 (2011) 592–595.
[13] F. Hayashi, K.D. Smith, A. Ozinsky, T.R. Hawn, E.C. Yi, D.R. Goodlett, J.K. Eng, S. Akira, D.M. Underhill, A. Aderem, The innate immune response to bacterial flagellin is mediated by Toll-like receptor 5, Nature 410 (2001) 1099–1103.
[14] L.G. Burdelya, V.I. Krivokrysenko, T.C. Tallant, E. Strom, A.S. Gleiberman, D. Gupta, O.V. Kurnasov, F.L. Fort, A.L. Osterman, J.A. Didonato, E. Feinstein, A.V. Gudkov, An agonist of toll-like receptor 5 has radioprotective activity in mouse and primate models, Science 320 (2008) 226–230.
[15] G. Liu, L. Song, L. Reiserova, U. Trivedi, H. Li, X. Liu, D. Noah, F. Hou, B. Weaver, L. Tussey, Flagellin-HA vaccines protect ferrets and mice against H5N1 highly pathogenic avian influenza virus (HPAIV) infections, Vaccine 30 (2012) 6833–6838.
[16] D.Y. Bargieri, D.S. Rosa, C.J. Braga, B.O. Carvalho, F.T. Costa, N.M. Espindola, A.J. Vaz, I.S. Soares, L.C. Ferreira, M.M. Rodrigues, New malaria vaccine candidates based on the *Plasmodium vivax* merozoite surface protein-1 and the TLR-5 agonist *Salmonella Typhimurium* FliC flagellin, Vaccine 26 (2008) 6132–6142.
[17] V. Le Moigne, G. Robreau, W. Mahana, Flagellin as a good carrier and potent adjuvant for Th1 response: study of mice immune response to the p27

(Rv2108) *Mycobacterium tuberculosis* antigen, Mol. Immunol. 45 (2008) 2499–2507.
[18] W.F. McDonald, J.W. Huleatt, H.G. Foellmer, D. Hewitt, J. Tang, P. Desai, A. Price, A. Jacobs, V.N. Takahashi, Y. Huang, V. Nakaar, L. Alexopoulou, E. Fikrig, T.J. Powell, A West Nile virus recombinant protein vaccine that coactivates innate and adaptive immunity, J. Infect. Dis. 195 (2007) 1607–1617.
[19] K.D. Smith, E. Andersen-Nissen, F. Hayashi, K. Strobe, M.A. Bergman, S.L. Barrett, B.T. Cookson, A. Aderem, Toll-like receptor 5 recognizes a conserved site on flagellin required for protofilament formation and bacterial motility, Nat. Immunol. 4 (2003) 1247–1253.
[20] M. Hong, S.I. Yoon, I.A. Wilson, Recombinant expression of TLR5 proteins by ligand supplementation and a leucine-rich repeat hybrid technique, Biochem. Biophys. Res. Commun. 427 (2012) 119–124.
[21] E. Andersen-Nissen, K.D. Smith, K.L. Strobe, S.L. Barrett, B.T. Cookson, S.M. Logan, A. Aderem, Evasion of Toll-like receptor 5 by flagellated bacteria, Proc. Natl. Acad. Sci. USA 102 (2005) 9247–9252.
[22] V.L. Campodonico, N.J. Llosa, M. Grout, G. Doring, T. Maira-Litran, G.B. Pier, Evaluation of flagella and flagellin of *Pseudomonas aeruginosa* as vaccines, Infect. Immun. 78 (2010) 746–755.
[23] G. Doring, C. Meisner, M. Stern, G. Flagella vaccine trial study, a double-blind randomized placebo-controlled phase III study of a *Pseudomonas aeruginosa* flagella vaccine in cystic fibrosis patients, Proc. Natl. Acad. Sci. USA 104 (2007) 11020–11025.
[24] E.T. Weimer, H. Lu, N.D. Kock, D.J. Wozniak, S.B. Mizel, A fusion protein vaccine containing OprF epitope 8, OprI, and type A and B flagellins promotes enhanced clearance of nonmucoid *Pseudomonas aeruginosa*, Infect. Immun. 77 (2009) 2356–2366.
[25] A. Kumar, N. Gao, T.J. Standiford, R.L. Gallo, F.S. Yu, Topical flagellin protects the injured corneas from *Pseudomonas aeruginosa* infection, Microbes Infect. 12 (2010) 978–989.
[26] Z. Otwinowski, W. Minor, Processing x-ray diffraction data collected in oscillation mode, Methods Enzymol. 276 (1997) 307–326.
[27] P.D. Adams, P.V. Afonine, G. Bunkoczi, V.B. Chen, I.W. Davis, N. Echols, J.J. Headd, L.W. Hung, G.J. Kapral, R.W. Grosse-Kunstleve, A.J. McCoy, N.W. Moriarty, R. Oeffner, R.J. Read, D.C. Richardson, J.S. Richardson, T.C. Terwilliger, P.H. Zwart, PHENIX: a comprehensive Python-based system for macromolecular structure solution, Acta Crystallogr. D Biol. Crystallogr. 66 (2010) 213–221.
[28] P. Emsley, K. Cowtan, Coot: model-building tools for molecular graphics, Acta Crystallogr. D Biol. Crystallogr. 60 (2004) 2126–2132.
[29] G.N. Murshudov, A.A. Vagin, E.J. Dodson, Refinement of macromolecular structures by the maximum-likelihood method, Acta Crystallogr. D Biol. Crystallogr. 53 (1997) 240–255.
[30] W. Hashimoto, J. He, Y. Wada, H. Nankai, B. Mikami, K. Murata, Proteomics-based identification of outer-membrane proteins responsible for import of macromolecules in *Sphingomonas* sp. A1: alginate-binding flagellin on the cell surface, Biochemistry 44 (2005) 13783–13794.
[31] Y. Maruyama, M. Momma, B. Mikami, W. Hashimoto, K. Murata, Crystal structure of a novel bacterial cell-surface flagellin binding to a polysaccharide, Biochemistry 47 (2008) 1393–1402.